Biochip reader with dynamic holographic excitation and hyperspectral fluorescence detection

Carsten Glasenapp
Wolfgang Mönch
Holger Krause
Hans Zappe
University of Freiburg
Department of Microsystems Engineering—IMTEK
Laboratory for Micro-optics
Georges-Köhler-Allee 102
Freiburg, BW 79110 Germany
E-mail: cg@glaspp.de

Abstract. A highly parallel microarray scanner for functional genomic research using a dynamically reconfigurable holographic excitation and hyperspectral fluorescence detection is described. The light from two laser sources (405 and 532 nm) is split into an arbitrary number of focused spots on the biochip using a pair of spatial light modulators and a novel imaging system. The parallel optical scanner includes a hyperspectral detection unit with a high-sensitivity CCD camera to detect and analyze the emitted fluorescence spectra (from 430 to 800 nm) of all illuminated spots simultaneously. By using an *xy* scanner, the spectra of all spots on an entire array can be read out line by line.
[DOI: 10.1117/1.2437143]

Keywords: holographic excitation; biochip; dynamic diffractive optical element; hyperspectral; liquid crystal; fluorescence.

Paper 05373RR received Dec. 19, 2005; revised manuscript received Sep. 9, 2006; accepted for publication Sep. 22, 2006; published online Jan. 30, 2007.

1 Introduction

The task of a biochip reader is to measure the intensity of light emitted from fluorescence-labeled biochemical species in the spots of a biochip that have been printed on a chemically surface-treated substrate.[1,2] A number of techniques have been developed during the last several years for this purpose.[1–9] These experimental approaches differ with respect to excitation mechanism (direct irradiation or via evanescent waves; single-spot, multispot, or full-area excitation) and detection technique (type of sensor; temporally, spatially, and/or spectrally resolved signals).

To obtain a high biochip throughput, full-area flood illumination of the fluorescence samples is often employed. Equipped with a CCD-based detection unit, diagnostic systems using this approach are rapid and cost-efficient.[3,4] Parallel readout of the biochip enables screening of many fluorescence samples simultaneously in a short time. Also, these systems are versatile with respect to the printing format of the biochips, i.e., they do not require a well-defined pitch of the spots of the microarray. On the other hand, a comparatively high level of background fluorescence significantly reduces their sensitivity.

Alternatively, highly sensitive fluorescence detection can be accomplished by excitation with a focused laser beam.[5] The fluorescence light from the spots is then detected by a photomultiplier tube (PMT), where the background fluorescence is reduced by a confocally mounted pinhole in front of the PMT. Here, an increased SNR enables an improved detection limit of the fluorescence light. Combined with fluorescence excitation by means of evanescent waves[6,7] (sometimes referred to as the total internal reflection fluorescence or TIRF), this method is capable of detecting even single fluorescent molecules.

However, to read out a complete microarray using the laser excitation approach, a mechanical scanning system is required because only one spot can be excited and read out at a time. Due to this sequential readout, the throughput of these systems is low.

Mehta et al.[8] and Blom et al.[9] demonstrated parallel fluorescence detection through multispot excitation using a laser-illuminated diffractive optical element. In this way, two essential advantages were realized: highly parallel excitation and an excitation only at the position of the spots of the biochip. Highly parallel multispot excitation increases the throughput of samples; excitation only at the position of the spots reduces background fluorescence from unbound marker molecules in the analyte surrounding the spots on the microarray, which means an increased excitation efficiency and improved SNR. However, when using static diffractive optical elements for holographic excitation, matching the diffraction pattern to the spot pattern requires additional imaging optics and mechanical translation stages. Therefore, the adaptation of the excitation unit to new spot patterns requires modification in the hardware of the setup.

Due to the availability of dynamic diffractive optical elements (D-DOEs), this limitation can now be overcome, such that arbitrarily pitched spot arrays can be excited without need for any further optical components. We present here a biochip reader that provides a means for dynamic holographic excitation in combination with a CCD-based hyperspectral detection unit for simultaneous fluorescence analysis at several wavelengths. The combination of these new technologies makes it possible to realize a high-throughput biochip reader with a high sensitivity and great versatility.

Address all correspondence to Carsten Glasenapp, Department of Microsystems Engineering, Laboratory for Micro-optics, Georges-Köhler-Allee 102, Freiburg, BW 79110 Germany; Tel: +497612037518; Fax: +497612037562; E-mail: cg@glaspp.de

1083-3668/2007/12(1)/014038/8/$25.00 © 2007 SPIE

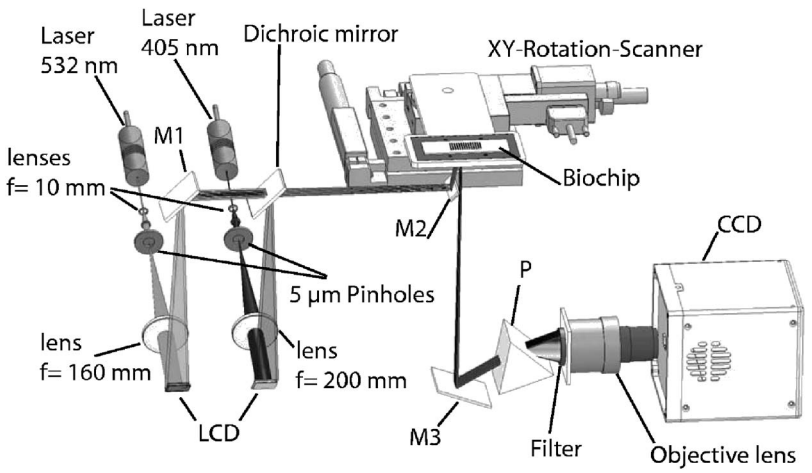

Fig. 1 Experimental setup for holographic excitation using two lasers and two LCDs; fluorescence detection for hyperspectral detection, consisting of filters for blocking the excitation light, a dispersive prism, and a highly sensitive CCD camera, equipped with a high-numerical-aperture objective lens. For the line-by-line scan and alignment of the biochip with respect to the excitation intensity pattern, a motorized *xy* translation stage and a motorized rotation stage is used in the setup.

2 Holographic Excitation

The basis of holographic excitation is a diffractive optical element (DOE), which is able to generate an arbitrary spatial phase modulation of an incoming lightwave. The appropriate phase modulation can generate a well-defined, 3-D modulation of the light intensity after reflection from or transmission through[10] the DOE.

The calculation of the required phase modulation for the DOE to achieve a desired arbitrary intensity profile is based on the reversibility of the light paths, i.e., light passes through an optical system backward in the same way as it does forward. Tracing back the light paths from the desired intensity distribution on the image plane (i.e., at the biochip) to the phase-shifting DOE enables the determination of the required phase shift to yield this intensity distribution.[11,12]

For adjustment of the pitch of the spot intensity pattern without replacement or mechanical movement of components, reflective liquid crystal displays [for example, a Hitatchi liquid crystal on silicon (LCoS) chip with 1280×1024 pixels] can be used as a D-DOE. The liquid crystal has an electric-field-dependent refractive index such that the refractive index of each cell of the LCoS display can be individually modified. The resulting spatial distribution of the refractive index causes a spatial phase modulation of the lightwave reflected from the LCoS display. Thus, for adaptation of the biochip reader to a new fluorescence spot pitch, only the calculation of the new phase modulation pattern of the D-DOE is required. The phase modulation pattern of the LCoS displays can be refreshed dynamically at a rate of 100 Hz, thereby enabling a linear movement or rotation or pitch adjustment of the intensity pattern at that rate.

3 Instrument Design

3.1 *Excitation Unit*

Figure 1 shows the optical setup for parallel holographic excitation. Two lasers illuminate two reflective liquid crystal displays (LCDs). The first, a 405-nm laser diode, has a maximum power of 25 mW (Chromalase 405, Blue Sky Research) and the second, a diode-pumped solid-state green laser, 32 mW at 532 nm (GLMC1-30). The intensity of both sources can be individually adjusted by the laser current. The two laser beams are expanded by two-beam expanders with confocal pinholes (5 μm) to fully illuminate the LCDs, which then modulate the phase of the incident light in a 2-D pattern as already described. The two separate light paths are joined together by mirror M1 and the dichroic mirror. A further mirror (M2) directs the modulated laser light through the biochip to excite the sample spots.

Generally, the rectangular aspect ratio of the LCDs leads to an asymmetric rectangular beam profile of the reflected light. To correct this asymmetry, the LCDs are illuminated under an oblique angle of incidence, which is given by the arccosine of the aspect ratio of the LCoS display. Then, the rectangular LCoS display appears quadratic to the incident beam, and the reflected beam has a square truncated Gaussian beam profile. At the same time, reflecting the circular expanded laser beam to a square beam profile is more efficient than reflecting it to a rectangular profile. Oblique illumination of the D-DOE also simplifies the optical setup, because no additional beamsplitters are required. On the other hand, oblique illumination requires a higher effort in the calculation of the holograms. First, the hologram must be stretched in one direction because of the projection onto the inclined plane of the LCD. Otherwise the focal spots would become astigmatic. Second, the varying distance from the LCD to the focal plane (i.e., the position of the biochip) must be taken into account because the LCD plane and the focal plane are not parallel. Based on these considerations, holograms were calculated with different spot distributions and pitches.[13] Figure 2(a) shows a calculated hologram for generation of 25 light spots with a pitch of 500 μm at a wavelength of 405 nm. Figure 2(b) (left and middle image) shows the type of aberrations, such as coma and astigmatism, which occur if the already-mentioned compensation for the oblique illumination of the D-DOE is not sufficiently considered in the hologram calculation. Finally, software-based full compensation of all effects resulting from

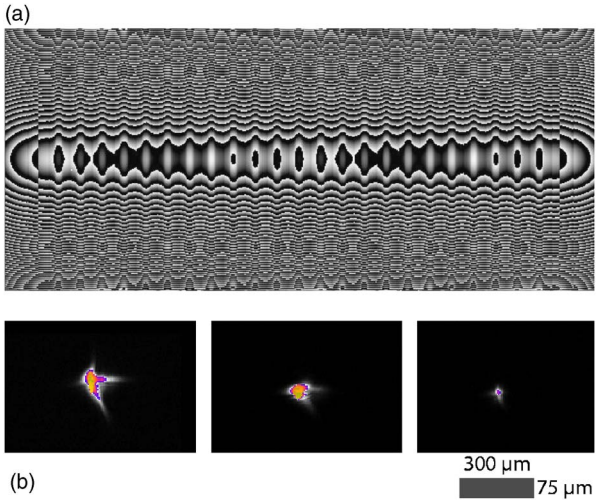

Fig. 2 (a) Hologram of 25 spots with compensation for oblique illumination (1280×640 pixels with a 13.7-μm pixel size) and (b) aberrations due to holograms with insufficient compensation of the oblique illumination of the DOE: left, astigmatism; middle, coma; and right, result of optimally compensated holographic structure.

oblique incidence leads to an optimized intensity profile of the spot [Fig. 2(b), right image].

By focusing the spot intensity pattern generated by the dynamic hologram onto a liquid fluorochrome film (rhodamine B, purchased from Fluka, dissolved in distilled water) sandwiched between a glass slide and a cover slide, the quality of the excitation unit was measured directly in the experimental setup. Hyperspectral detection of the fluorescence light does not provide an image of the spots, but rather an exact determination of the intensity of each spot. Figure 3(a) shows an image plane cross section of 21 spots generated with a D-DOE at a wavelength 405 nm. The contrast between bright and dark zones is 0.93, and the standard deviation of the intensity maximum over the 21 foci is 10%. The truncated Gaussian intensity distribution of the incident light is the reason for the smaller intensity in the last two spots on the left side. Under consideration of the light intensities of each spot, the evaluation software can determine the dye concentration from the measured fluorescence intensity of each fluorescence sample. Figure 3(b) shows a picture of 10 excitation spots imaged directly onto a CCD sensor in the focal plane, i.e., at the position of the biochip.

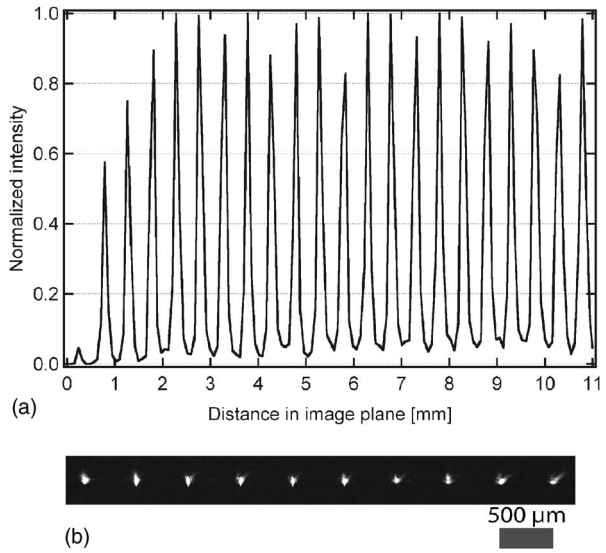

Fig. 3 (a) Intensity profile of a 1-D array of 21 focused spots generated with a D-DOE, where the intensity per spot is 10 μW, the beam diameter in the focal plane is 160 μm, the pitch is 500 μm, and the pixel pitch of the D-DOE is 13.7 μm, (b) and image of 10 focused spots on the CCD sensor.

3.2 *Detection Unit*

The fluorescence light emitted from a thus excited line of spots is imaged onto a CCD sensor (a 2-D object), with one coordinate on the CCD for the spatial information (i.e., which spot in the row) and the other coordinate for the spectral information from the fluorescence light of that spot.[14] The essential elements of this hyperspectral detection unit, as seen in Fig. 1, are a dispersion prism (P) for spectral separation, a highly sensitive CCD-camera (SamBa SE-34; Sensovation AG; 658×496 7.4-μm square pixels with 12-bit resolution), a special filter set (see later in the paper), and an objective lens with high numerical aperture (Schneider-Kreuznach Xenon 25/0.95).

Lateral magnification, i.e., the size of the imaged spot on the CCD sensor is an important issue in hyperspectral detection. A high lateral magnification M leads to a high spatial resolution of detected signals and the number of illuminated pixels for a spot increases quadratically with M as can be seen from

$$N = M^2 \frac{D^2 \pi}{4P^2}, \tag{1}$$

where N is the number of illuminated pixels, D is the diameter of the spot, P is the width of the CCD pixel, and M is given by

$$M = \frac{\text{image size on CCD chip}}{\text{spot size on biochip}}. \tag{2}$$

Each pixel requires a minimum number of photons to provide a signal level significantly larger than the thermal background noise. For reliable detection, the number of illuminated pixels per spot and, therefore, the image magnification should not be too high. Furthermore, along with a lower magnification, the solid angle of the collected fluorescence photons is reduced. The intensity of the collected light can be calculated from

$$I_{\text{collected}} = \frac{1}{16 f\#^2} \frac{M^2}{(1+M)^2}, \tag{3}$$

where $f\#$ is the f-number of the objective lens. Dividing Eqs. (1) and (3) gives the intensity collected for 1 pixel:

$$I_{\text{per pixel}} = \frac{I_{\text{collected}}}{N} = \frac{P^2}{4\pi D^2 f\#^2} \frac{1}{(1+M)^2}. \tag{4}$$

As we can see from Eq. (4), the intensity per pixel decreases with increasing magnification M. At small M the right part of

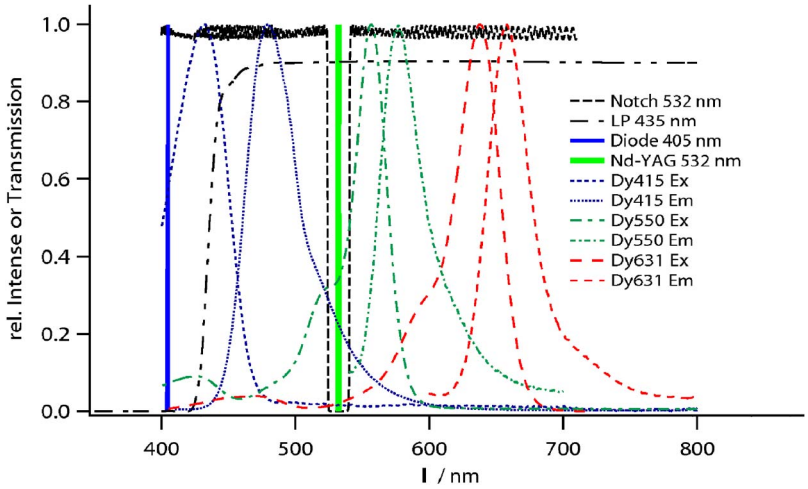

Fig. 4 Emission (Em) and excitation (Ex) spectra of the fluorochromes Dy415, Dy550, and Dy631; the laser lines used are 405 and 532 nm; and the transmission spectra of the low-pass (LP) and notch filters.

Eq. (4) converges toward unity, but the number of illuminated pixels also decreases rapidly.

For these reasons, the lateral magnification has to be optimized such that a reasonable number of pixels (10 to 100) is illuminated and the intensity per pixel is sufficiently high for reliable detection.

The typical spectral width of a fluorochrome emission spectrum is[15] about 50 nm. Therefore, to distinguish five different fluorochromes in the range of 430 to 800 nm with this detection unit, a spectral resolution of 10 nm is sufficient. Furthermore, a spatial resolution of about 100 μm is sufficient for measurement of a microarray with a pitch of 500 μm. Using these values, and with a pixel size of the used CCD sensor of 7.5 μm, we calculated an optimal magnification $M=10$.

Although they are frequently used in spectrometers, the overall performance of diffraction gratings turned out to be inferior when compared to the dispersive prism used here, due to their strongly wavelength-dependent diffraction efficiency. An antireflection-coated, 50-mm BK7 prism proved to have superior performance and was thus used for spectral separation. Depending on the dispersive power of the prism, its position in the optical path, the pixel pitch of the CCD detector and the objective lens, the detection unit achieved a spectral resolution of 8 nm in the red, 5 nm in the green, and 2 nm in the blue regions of the spectrum.

The spatial resolution of the system is 80 μm, sufficient to resolve the printed DNA spots of the microarray. A printed spot with a diameter of 300 μm is imaged to 3 pixels in the spatial axis of the CCD sensor, and to 6 to 20 pixels in the wavelength axis, the latter depending on the wavelength range. As we can see from Fig. 7 in Sec. 5 this pixel number is sufficient to resolve the spectra of all fluorochromes used. As a further advantage of hyperspectral detection over detection in a small spectral range (as is done using interference filters), detection of the full emission spectra of the spots allows the discrimination of the fluorescence signals of the spots and that of the background (mostly emitted from the substrate).

3.3 *Filters*

The fluorescence emission peak is shifted towards longer wavelengths ("Stokes shift") with respect to the excitation wavelength;[15] this shift is typically about 20 nm. To detect weak fluorescence signals, the excitation wavelength must thus not reach the detection unit, such that efficient filters for blocking the excitation light are required.

In the setup of Fig. 1 a special filter combination is used to measure the fluorescence of different sets of fluorochromes. A 435-nm long-pass filter (Schott Glas; GG435) blocks the shortest excitation laser wavelength (405 nm), and a notch-filter (Semrock StopLine™ 532.0) with an optical density higher than 10^6 at 532 nm blocks the second excitation laser line at 532 nm. With this combination of filters, most fluorochromes in the visual spectrum can be detected. The blue and green fluorochromes can be stimulated with the near-UV light of the blue laser. To stimulate green and red fluorochromes, the laser at 532 nm can be used. Figure 4 illustrates the transmission spectra of the filters employed in relation to the two laser lines as well as the emission and excitation spectra of the three fluorochromes, Dy415, Dy550, and Dy631.

3.4 *Automation*

To measure complete microarrays, the entire system was computer controlled. Several parameters, such as the spot grid, the integration time of the CCD, or the spectral and spatial range, can be dynamically altered. Thus, the use of different biochips with differing array pitches does not require hardware changes since the holographic excitation pattern is defined purely by software.

In a typical measurement, a manual visual alignment of the microarray via the CCD image is necessary before a readout sequence can be started. During the microarray scan, a hardware-based handshake between the motorized stepper, the CCD camera, and the lasers controls the readout. After moving the microarray to the appropriate line of spots to be

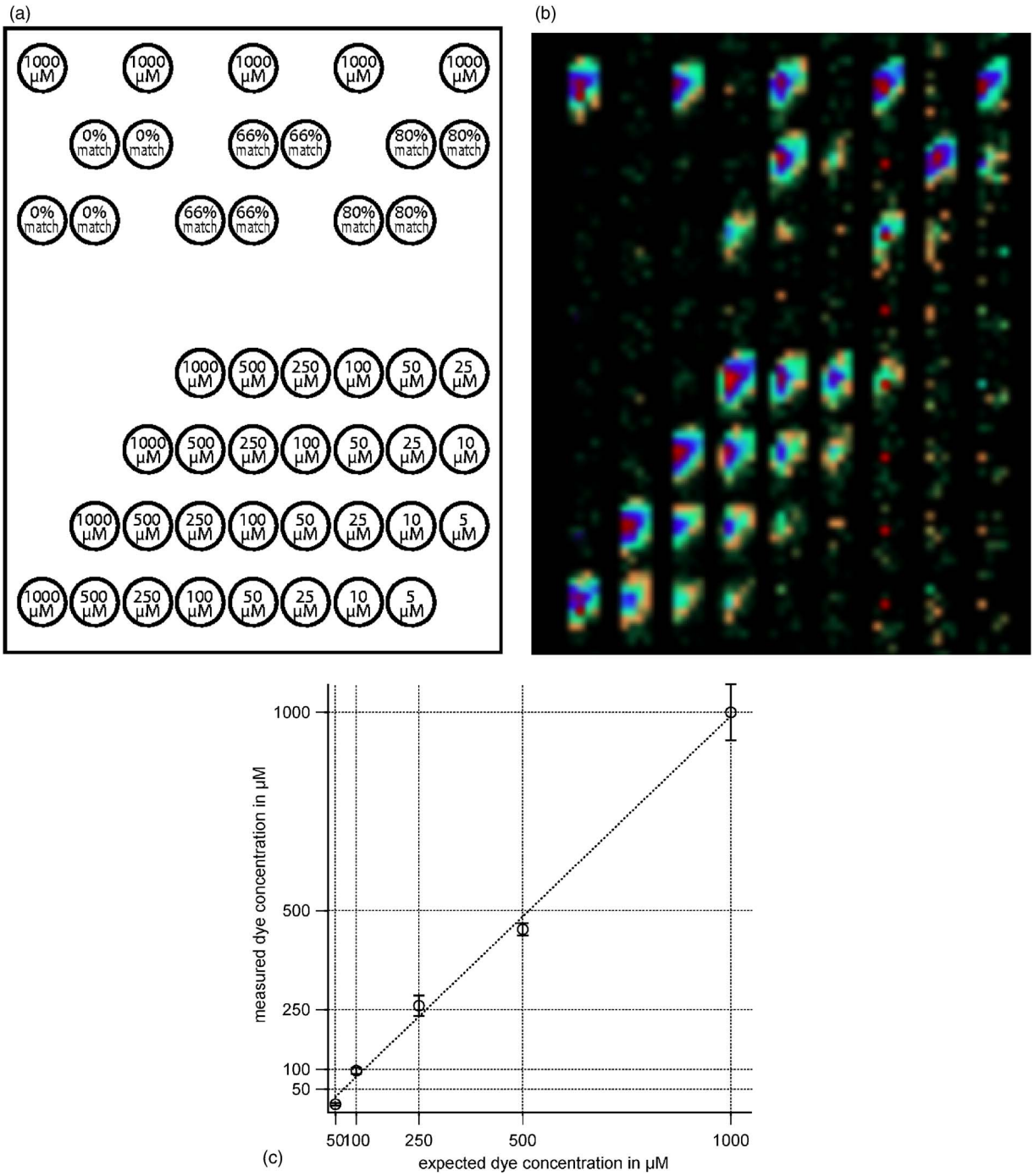

Fig. 5 Detection of oligonucleotide concentrations at several concentrations: (a) test chip configuration with 500-μm spot grid, including reference spots (line 1); hybridization test-spots with different match-mismatch constellation (lines 2 and 3) and oligonucleotide concentrations from 1000 to 50μM (remaining lines); on one chip 4×4 of these subareas are printed; (b) with the system measured image of one subarea of the test chip; and (c) integrated fluorescence signal of the four concentration lines with varying nucleotide concentrations showing the linear dependence of the fluorescence signal on the dye concentration.

measured, the motion controller sends a signal to the camera to start the data acquisition. The two lasers are switched on by the camera only during data acquisition such that the photobleaching of the organic fluorochromes is kept to a minimum. After the measured data from the camera are received, the program starts the motion controller again to read out the next line of the microarray and this procedure is repeated until the full microarray is read out.

For most measurements, an integration time of 1 s is sufficient but for more sensitive detection, a longer integration

time can be chosen. Integration times longer than 10 s are unsuitable, however, since the background noise due to the dark current of the CCD begins to dominate the signal. Consequently, the readout of a standard microarray slide of 75 $\times$25 mm with an array pitch of 500 μm takes about 150 to 1500 s for about 3000 single spots.

4 Quantitative Concentration Measurement

To quantify the performance of the system, a DNA-based test chip was employed. On an amino-silane-coated glass slide (GAPS™ II, Corning), a microarray with different oligonucleotide concentrations was printed. The format of the chip was 25$\times$75 mm and the distance between the spots 500 μm; a standard VHL sense-strand oligonucleotide (SVSO) was used. Concentrations from 1000 to 5 μM (M=mol/l) were printed with a high precision needle printer on the slides. After washing, UV crosslinking and drying, the slides were hybridized for 16 h at 42 °C with 100 mM SVSO-FL-Cy3 fluorescence labeled oligonucleotide solution. The slides were subsequently washed and dried again.

To verify the hybridized oligonucleotide concentrations, the chip was first examined with two commercial biochip readers, an Axon GenePix® 4000 and a GeneScan Biodetect 645/4. The Axon reader, with photomultiplier detection, was able to detect all concentrations (5 to 1000 μM) with a resolution of 10 μm in 240 s. The CCD-based reader (GeneScan) detected the concentrations from 1000 down to 50 μM with an integration time of 90 s.

Figure 5(a, top) shows a picture of the area of the test chip measured with the system developed here. With an illumination power of 15 μW per spot, the chip was read out line by line using holographic excitation. The exposure time of each line was 1 s. The readout of the 4$\times$4 subareas shown in Fig. 5 took 80 s in total (2 s for the whole readout of one line). After integration of the fluorescence signal of each spot the signal shows the correspondence between the measured fluorescence intensity and the oligonucleotide concentration. As seen in Fig. 5(c), the system was able to measure oligonucleotide concentrations from 1000 down to 50 μM with a linear dependence between the dye concentration and the fluorescence intensity. In spite of the hyperspectral evaluation, which decreases the sensitivity of the detection by the distribution of the fluorescent light on more camera pixels, the same sensitivity as the commercial CCD-based microarray reader is attained,[16] showing that implementation of hyperspectral detection in microarray biochip readers may not necessarily adversely affect performance.

Both CCD-based systems showed a reduced SNR at longer integration times due to a strong increase of the background noise caused by the autofluorescence of the slide and the dark current noise of the CCD. To minimize the autofluorescence of the slide, we used amino-silane-coated glass slides, which showed a much lower autofluorescence compared to TOPAS® and PMMA plastic slides. The dark current noise of the CCD camera can be reduced by cooling the CCD chip. To detect lower concentrations than those demonstrated here, the use of a cooled CCD camera is reasonable and with this technology the system could lead to sensitivities comparable to a photomultiplier-based system.

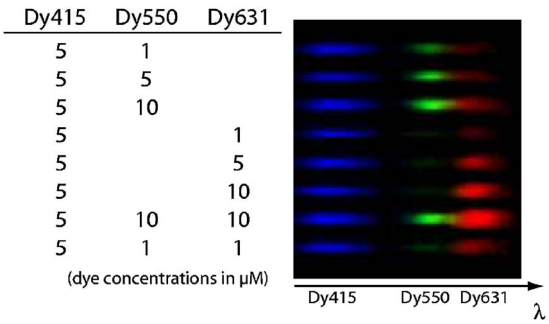

Fig. 6 Hyperspectral picture of a multicolored test biochip. The image shows eight spots with different dye mixtures of Dy415 (blue), Dy550 (green), and Dy631 (red). The horizontal axis corresponds to the wavelength. The table on the left illustrates the dye-mixture of each spot.

5 Detection of Emission Spectra

Modern biochips are able to assay complex biochemical reactions. To obtain more information from a single spot, several fluorochromes are frequently used simultaneously.[1] This requires a biochip reader capable of a detailed spectral analysis of the fluorescence signal to discriminate different fluorochromes, one motivation for the hyperspectral detection unit presented here.

To evaluate the performance of the microarray scanner, a test system with the fluorochromes Dy631 (red), Dy550 (green), and Dy415 (blue) (Dyomics GmbH) was made. Different mixtures of these dyes were spotted onto a glass slide using a commercial needle printer. As we can see in Fig. 6, the hyperspectral detection unit can measure the fluorescence intensity of the three different dyes simultaneously. The color picture illustrates the spectral distribution of each spot of the microarray biochip and a qualitative correlation between the concentrations and the intensity of the fluorescence signal can be observed. Figure 7 shows the measured fluorescence intensities versus the wavelength for different dye mixtures; in each case, the spectrum of the individual dyes is also shown for comparison. By comparing the fluorescence spectra of the spots with the known spectra of the fluorochromes employed, evaluation of the spectra may be used to determine the dye concentrations. It is clear in the figure that the fluorescence intensity peaks correspond to the dye concentrations.

In addition, the different fluorescence intensities measured for identical concentrations of different dyes is due to the different quantum efficiencies of the dyes. As we can see in Figs. 7(a) and 7(b), the fluorescence intensity of the red fluorochrome Dy631 is nearly the same as that of the Dy550 (green), even though the excitation with the green laser at 532 nm is not optimal for Dy631. The results also show that excitation with the two lasers at 405 and 532 nm is sufficient to excite all three fluorochromes at the same time. However, if red dyes are extensively employed, the use of a third red laser source would be preferable.

Figure 7(c) shows the spectral distribution of two spots with three different dyes. In this case, the fluorescence intensity of the green dye is less than the intensity of the red dye. This dimming of the green fluorescence intensity is caused by the fluorescence resonance energy transfer (FRET) from the

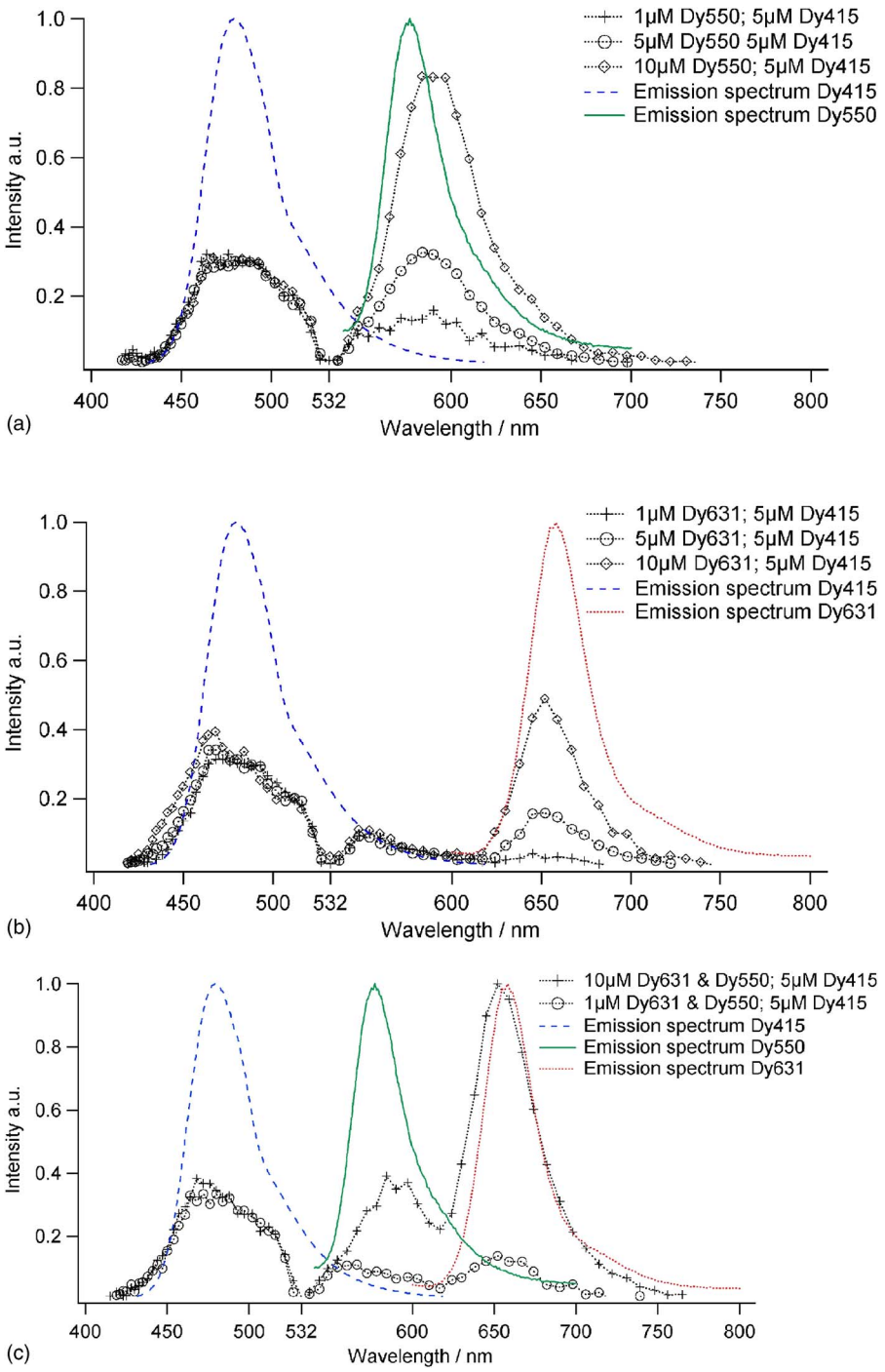

Fig. 7 Emission spectrum of multicolored spots illuminated with 405 and 532 nm. The plots show the measured data and the native spectra of the corresponding fluorochromes: (a) three emission spectra of spots with Dy415 and Dy550 at different mixtures, (b) three emission spectra of spots with Dy415 and Dy631 at different mixtures, and (c) two emission spectra of three color spots at different mixtures. The minimum at 532 nm is caused by the notch filter used as a wavelength reference.

green to the red fluorochrome, as described by Förster[17] in 1948.

6 Conclusion

A new approach for highly parallel hyperspectral fluorescence spectroscopy using holographic excitation of a microarray biochip was presented. A key feature of the instrument is the flexible, multipoint excitation of fluorescence spots using spatial light modulators. This new approach has four notable advantages. First, due to the holographic multipoint illumination, excitation light is focused only onto the spots under investigation; background fluorescence is thereby reduced and the measurement shows a higher contrast when compared to flood illumination. Second, an adaptation to arbitrary spot

configurations can be achieved by changing the holograms by software modification only; modifications of the hardware are not required. Third, parallel illumination and readout of 1-D spot arrays increase the throughput compared to single-point scanning techniques. Finally, continuous spectral fluorescence detection enables discrimination of various dyes without modification of the optical setup, providing additional information on the chemical reactions that take place on the biochip and increasing the sensitivity by eliminating significant background fluorescence. The presented system thus represents a fast, universal, and reliable prototype biochip readout unit and enables high throughput complex DNA detection.

Acknowledgments

This work was funded by MOBA (Micro-Optical Biochip Analysis) as part of the research program Biophotonik 1 of the German Ministry of Education and Research (BMBF). We gratefully acknowledge cooperation and support from Sensovation AG (Stockach, Germany) and the assistance of Dipl.-Chem. Thorsten Neumann (IMTEK, Laboratory for Chemistry and Physics of Interfaces).

References

1. M. Schena, *Microarray Biochip Technology*, Eaton Publications, Natick, MA (2000).
2. P. Baldi and G. Wesley Hatfield, *DNA Microarrays and Gene Expression*, Cambridge University Press, Cambridge (2002).
3. F. J. Steemers, J. A. Ferguson, and D. R. Walt, "Screening unlabled DNA targets with randomly ordered fiber-optic gene arrays," *Nat. Biotechnol.* **18**, 91–94 (2000).
4. G. Valentini and C. D'Andrea, "Time-resolved DNA-microarray reading by an intensified CCD for ultimate sensitivity," *Opt. Lett.* **25**, 1648–1650 (2000).
5. W. Denkl, D. W. Piston, and W. W. Webb, in *Handbook of Biological Confocal Microscopy*, Ed., J. B. Pawley, Plenum Press, New York (1990).
6. W. M. James, C. Gu, and M. Gu, "Scanning total internal reflection fluorescence microscopy under one-photon and two-photon excitation, image formation," *Appl. Opt.* **43**, 1063–1071 (2004).
7. H.-P. Lehr, A. Brandenburg, and G. Sulz, "Modeling and experimental verification of the performance of TIRF-sensing systems for oligonucleotide microarrays based on bulk and integrated optical planar waveguides," *Sens. Actuators B* **92**, 303–314 (2003).
8. D. S. Mehta, C. Y. Lee, and A. Chiou, "Multipoint parallel excitation and CCD-based imaging system for high-throughput fluorescence detection of biochip micro-arrays," *Opt. Commun.* **190**, 59–68 (2001).
9. H. Blom, M. Johansson, and A. S. Hedmann, "Parallel fluorescence detection of single biomolecules in microarrays by a diffractive-optical-designed 2×2 fan-out element," *Appl. Opt.* **41**, 3336–3342 (2002).
10. L. B. Lesem, P. M. Hirsch, and J. A. Jordan Jr., "The Kinoform, A new wavefront reconstruction device," *IBM J. Res. Dev.* **13**, 150–155 (1969).
11. M. W. Farn, "New iterative algorithm for the design of phase only gratings," in *Computer and Optical Generated Holographic Optics*, I. Cindrich and S. H. Lee, Eds., *Proc. SPIE* **1555**, 34–42 (1991).
12. J. W. Goodman, *Introduction to Fourier Optics*, 2nd ed. (McGraw-Hill, New York 1996).
13. C. Glasenapp, W. Mönch, H. Krause, and H. Zappe, "Optical systems for fluorescence analysis," in *Biophotonics, Visions for Better Health Care*, J. Popp and M. Strehle, Eds., pp. 421–433, Wiley-VCH, Weinheim (2006).
14. R. A. Schultz, T. Nielsen, J. R. Zavaleta, R. Ruch, R. Wyatt. and H. R. Garner, "Hyperspectral imaging, a novel approach for microscopic analysis," *Cytometry* **43**, 239–247 (2001).
15. S. Svanberg, *Atomic and Molecular Spectroscopy*, 2nd ed., Springer Verlag, Berlin (1992).
16. M. B. Sinclair, J. A. Timlin, D. M. Haaland, and M. Werner-Washburne, "Design, construction, characterization, and application of a hyperspectral microarray scanner," *Appl. Opt.* **43**, 2079–2088 (2004).
17. T. Förster, "Intermolecular energy migration and fluorescence," *Ann. Phys.* **2**, 55–75 (1948).